# PV system control simulation and stability using lypunov theory

**Ahmed A. Farahat[1], Azza A. ElDesouky[2]andGamal. A. Mahmoud[2]**

*1 Company of East Delta for Electricity Production*

*2 Department of Electrical Engineering*

*Faculty of Electrical Engineering*

*Port-Said University*

*Port Fouad 42523, Port Said, Egypt*

***Abstract-*** With the pervasion and remarkable increase of PV' penetration on power system, the study of the leverage of its stability has become more urgent. Therefore, a modified control methodology of three phase grid connected PV system at different solar radiation and temperature is introduced in this paper. This include the design of a modified algorithm of incremental conductance to produce the maximum power point (MPP) and a control strategy of full decoupled current for grid is observed in rotating d-q synchronous reference frame for mutating the maximum power to AC power. Then, the Lyapunov function analyze the stability of the photovoltaic system under different operating conditions with another view. Moreover, a modified dynamic stability based on zero dynamic control design approach of feedback linearization is set. Simulation results on MATLAB/Simulink software simulate the effectiveness of the proposed control scheme in terms of delivering maximum power into the grid under varying atmospheric conditions.

Index Terms-PV system, maximum power point, PV control, dynamic stability, Lyapunov function

## I. INTRODUCTION

One of the most auspicious renewable energy sources is the solar energy due to the abundance of solar insulation in various regions, low operation and maintenance costs. However, solar energy is intermittent, depending upon weather conditions [1 2].

Many control strategies and controller types [3 4] have been investigated. PV system utilize Two control stages for connected grid. In all conditions, the utmost object of PV system control is to get the best values of current and voltage to put PV system at the maximum power. The maximum power point tracking (MPPT) methods are designed that diverge in implementation complexity, convergence speed, sensed parameters and cost, range of operation, popularity and their application [5 6].The incremental conductance (INC) is the most commonly algorithm utilized as it is suitable for the rapid change in atmospheric conditions. However, it requires a relatively harsh detection devices and the choice of the step and threshold is also more stressful [7 8].The second control stage is a current controlled sinusoidal PWM in d-q synchronous frame, which sets the DC link voltage of the inverter at a constant reference value as well as controls the active and reactive currents injected into the grid [9].



The main objective of this paper is to examine the control and stability of the operation of PV generation under different operation conditions. The lyapunov function is robust and effective to analyze the system stability. Therefore, a dynamic stability of the PV systems using an approach based on the formulation of the Lyapunov function is introduced [10].Moreover, a modified zero dynamic design approach of feedback linearization is proposed. It algebraically linearized the system and therefore a linear controller can be designed [11].

The rest of the paper is organized as follows. The mathematical model of a PV system is shown in the following section. Section 3 presents different controls for a three-phase grid-connected photovoltaic system. Dynamic stability analysis using Lyapunov function method is proposed in section 4. The simulation results with the proposed controllers under different circumstances are shown in section V.

## II. MODELING OF THE PV SYSTEM

The ideal photovoltaic module is represented as a single diode connected in parallel with a light generated current source ($I_{pv,cell}$ ) as shown in Fig. 1[12 13]. The output current is given by:

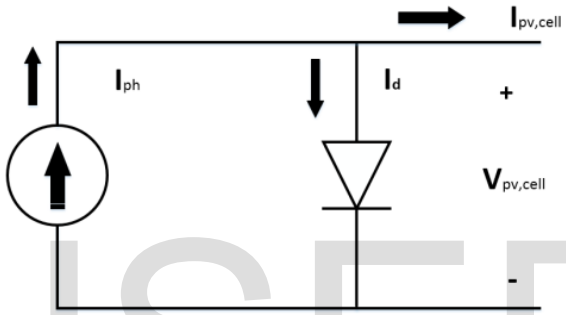


Fig. 1The ideal PV cell



$$I_{pv,cell} = I_{ph,cell} - I_{d,cell} \quad (1)$$

$$I_{pv,cell} = I_{ph} - I_0 \left[ exp\left(\frac{qV_{pv,cell}}{KT_cA}\right) - 1 \right] \quad (2)$$

$$T_c = T_A + \frac{G(NOCT-20)}{800} \quad (3)$$

Where $I_{ph,cell}$ is the current generated by the incident light which is directly proportional to the sun irradiation,$I_{d,cell}$ is the Shockley diode equation, $I_0$ is the reverse saturation or leakage current of the diode, $q$ is the electron charge (1.60217646 × 10−19 C), $K$ is the Boltzmann constant (1.3806503 × 10−23 J/K), $T_c$(in Kelvin) is the temperature of the cell [14], $T_A$ is the ambient temperature in Kelvin , G is the

radiation in W/m$^2$ and NCOT is the normal cell operating temperature , $A$ is the diode ideality constant and $V_{pv,cell}$ is the output voltage of cell.

However, practical arrays are composed of several connected PV cells and therefore, additional parameters should be included to the basic equation. Fig. 2 shows a more practical PV model, where $R_s$ and $R_p$ are the equivalent series and parallel resistance of module, respectively.

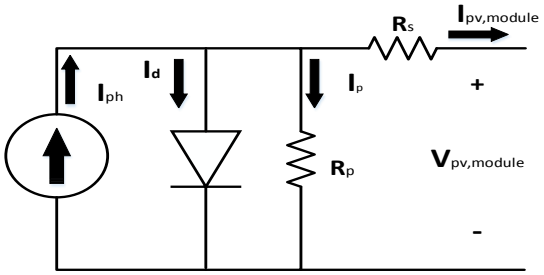


Fig. 2 Model of the PV module

$$I_{pv,module} = I_{ph} - I_0\left[exp\left(\frac{V_{pv,module}+I_{pv,module}R_s}{V_tA}\right)-1\right] - \frac{V_{pv,module}+I_{pv,module}R_s}{R_p} \quad (4)$$

Where $V_t = \frac{N_s K T_c}{q}$ and $N_s$ are the number of series cells on the module

It is assumed that $I_{sc} \approx I_{ph}$ as in practical devices the series resistance is low while the parallel resistance is high. Where $I_{sc,n}$ is the nominal short circuit current. The light-generated current of the PV cell depends linearly on the solar irradiation and is also influenced by the temperature as [15]

$$I_{ph} = \{I_{ph,n} + K_I[T_c - T_n]\}.\frac{G}{1000} \quad (5)$$

Where $I_{ph,n}$ is the light-generated current (in amperes) at the nominal condition (usually 25 ◦C and 1000 W/m$^2$), $T_c, T_n$ are the actual and nominal temperatures [in Kelvin], respectively and $K_I$.is the cell's short circuit current temperature coefficient in A/◦C.

The diode saturation current $I_0$depends on the temperature and is expressed as

$$I_0 = I_{0,n}\left(\frac{T_n}{T_c}\right)^3 exp\left(\frac{qE_g}{KA}\left(\frac{1}{T_n}-\frac{1}{T_c}\right)\right)$$

(6)

Where $E_g$ is the band gap energy of the semiconductor ($E_g$ =1.12 eV for the polycrystalline Si at 25 ˚C), and $I_{0,n}$ is the nominal saturation current and is expressed by the following equation

$$I_{0,n} = \frac{I_{sc,n}}{\exp\left(\frac{V_{oc,n}}{AV_{t,n}}\right)-1}$$

(7)

Where $V_{oc,n}$ , $V_{t,n}$ are the nominal open-circuit voltage and the thermal voltage of $N_s$ series-connected cells at the nominal temperature $T_n$. At very high temperature Eq.(5) is replaced with the following

$$I_0 = \frac{I_{sc,n}+K_I[T_c-T_n]}{\exp\left(\frac{V_{oc,n}+K_V[T_c-T_n]}{AV_{t,n}}\right)-1}$$

(8)

In the case of PV system, the effect of $N_p \& N_s$ are take into consideration. Then the output current of PV system is represented as:

$$I_{pv} = N_p I_{ph} - N_p I_0\left[exp\left(\frac{V_{pv}+\frac{N_S}{N_p}IR_S}{V_t A N_S}\right)-1\right]-\frac{V_{pv}+IR_S\frac{N_S}{N_p}}{R_p\frac{N_S}{N_p}}$$

(9)

Where $V_{pv}$ is the output voltage of the PV system and $N_p$ parallel cells on PV system .

## III. THE CONTROL OF PV SYSTEM

Fig 3 shows two control stages that are employed for grid connected PV system. The first stage is the boost converter, which will raise the relatively low solar voltage to a level suitable for the dc link directly connected to the inverter. The second stage is the DC to AC inverter that injects unity power factor current

to the grid. The duty of the inverter is to supply a continuous power from the dc link bus to a three phase utility line through a filter to reduce the ripple components due to PWM switching operation [16].

## A. MPPT Control

The INC comes from the fact that it uses the derivative of the PV system conductance, in order to determine the operating point position in relation to MPP. In this work, a modified INC algorithm is modified in order to include an integral regulator. The integral regulator minimizes the error $(\frac{\partial I_{pv}}{\partial V_{pv}} + \frac{I_{pv}}{V_{pv}})$ where the regulator output equals duty cycle correction [17]. The power output from the solar PV array is

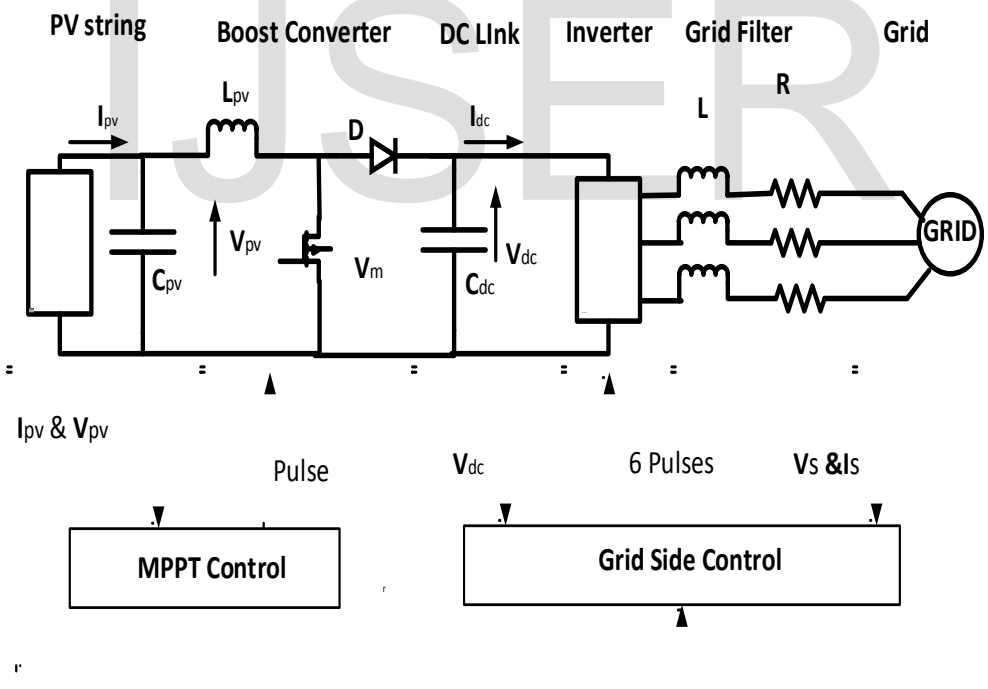


Fig. 3 General diagram of grid connected photovoltaic system

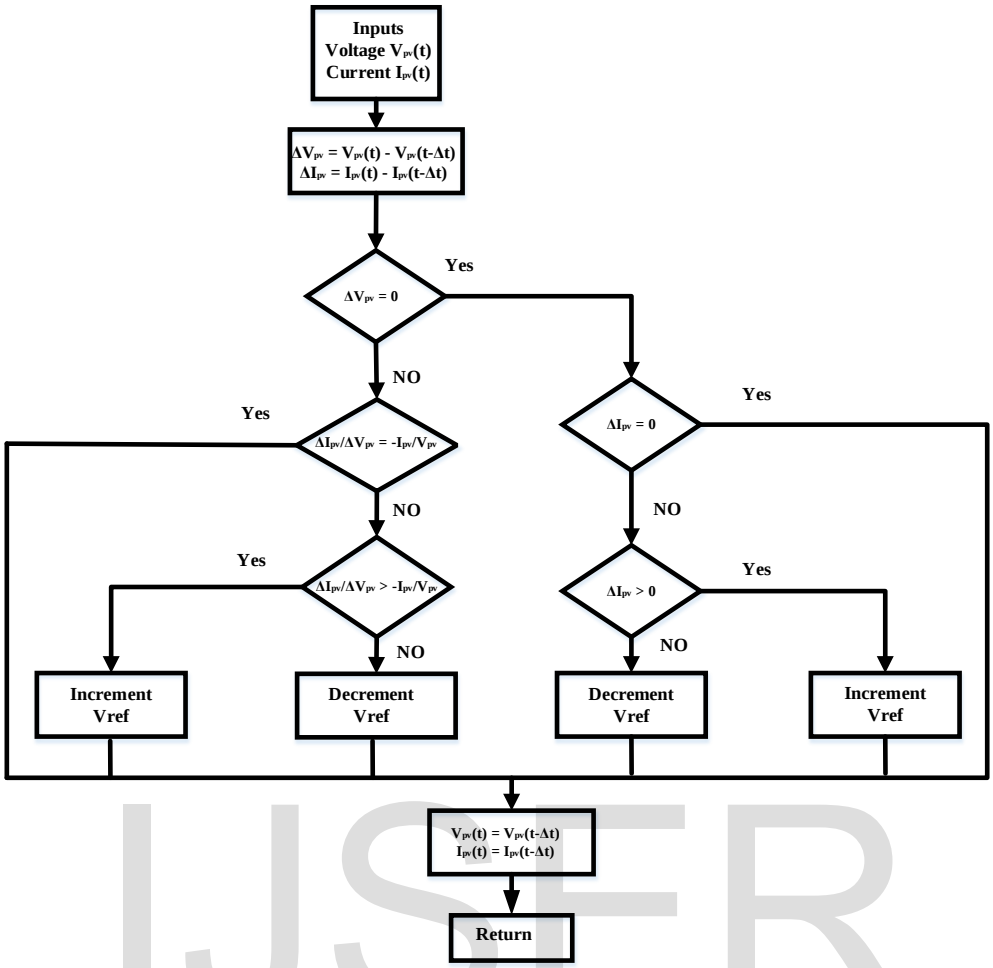


Fig. 4 the incremental conductance method of MPPT

$$P_m = V_{pv} I_{pv} \quad (10)$$

Maximum power point is obtained when $\frac{\partial I_{pv}}{\partial V_{pv}} = 0$

$$\frac{\partial P_m}{\partial V_{pv}} = \frac{\partial (V_{pv} * I_{pv})}{\partial V_{pv}} = V_{pv} * \frac{\partial I_{pv}}{\partial V_{pv}} + I_{pv} \quad (11)$$

$$\begin{Bmatrix} \frac{\partial P_m}{\partial V_{pv}} > 0 \ \ if \quad \frac{I_{pv}}{V_{pv}} > -\frac{\partial I_{pv}}{\partial V_{pv}} & \text{on the left of the MPP} \\ \frac{\partial P_m}{\partial V_{pv}} = 0 \ \ if \quad \frac{I_{pv}}{V_{pv}} = -\frac{\partial I_{pv}}{\partial V_{pv}} & \text{at the MPP} \\ \frac{\partial P_m}{\partial V_{pv}} < 0 \ \ if \quad \frac{I_{pv}}{V_{pv}} < -\frac{\partial I_{pv}}{\partial V_{pv}} & \text{on the right of the MPP} \end{Bmatrix}$$

(12)

Where $P_m$ is the maximum power of the PV system.

A controller is added in order to improve the INC method by minimizing the error between the actual and the incremental conductance. The flowchart of this method is shown in Fig. 4.



### B. Grid Side Control

The switching functions of the converters, inverters and the intermittency of the sunlight causes the nonlinearities of the grid-connected PV systems. A modified zero dynamic design approach of feedback linearization is used to control the grid current and dc link voltage. The modified approach linearizes the system partially and enables to design a linear controller for reduced order photovoltaic systems as shown in Fig. 5 [9 11]. As compared to the model in [11], the work presented herein offers the following distinguishing contribution: (1) a boost converter is used for matching the load impendence with the internal impendence of the string by adjusting duty ratio provided from MPPT algorithm, (2) The MPPT controls the boost converter to get the reference values for grid controller (Eq. 17 & Eq.18) with different PI controller values. The following equations are conducted from Fig. 5

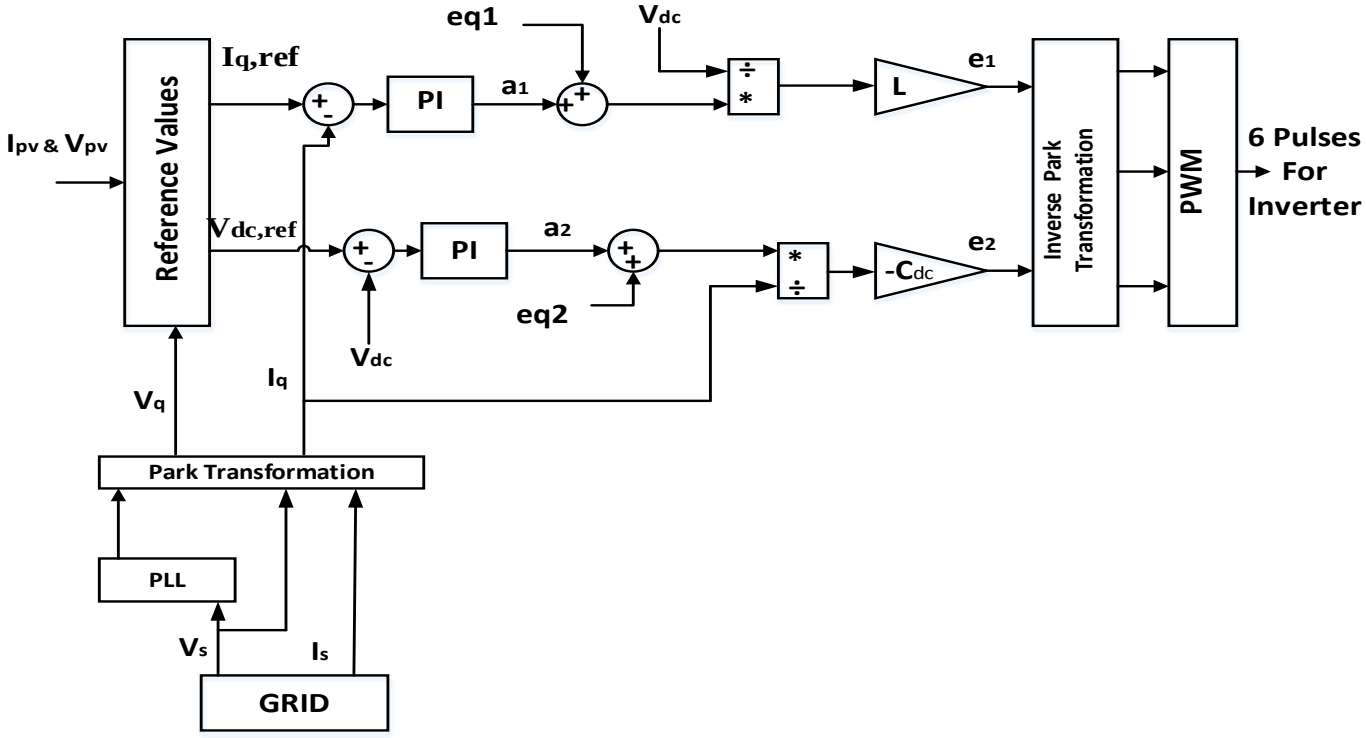


Fig. 5 Grid side control



$$e_1 = \frac{L}{V_{dc}}(a_1 + eq_1)$$

(13)

$$e_2 = -\frac{C_{dc}}{I_q}(a_2 + eq_2)$$

(14)

$$a_1 = k_{p1}\left(I_{q,ref} - I_q\right) + k_{I1}\int\left(I_{q,ref} - I_q\right)dt$$

(15)

$$a_2 = k_{p2}\left(V_{dc,ref} - V_{dc}\right) + k_{I2}\int\left(V_{dc,ref} - V_{dc}\right)dt$$

(16)

$$eq_1 = \omega I_d + \frac{R}{L}I_q + \frac{V_q}{L}$$

(17)

$$eq_2 = \frac{I_{dc}}{C_{dc}} - \frac{LI_d}{C_{dc}V_{dc}}(a_1 + \omega I_d + \frac{R}{L}I_q + \frac{V_q}{L})$$

(18)

where $e_1$&$e_2$ are the input of the PWM, $V_{dc}$&$I_{dc}$ are the output voltage and current of boost converter, d & q referee to direct and quadrant axies, $a_1$&$a_2$ are the output of PI control of grid side control, R&L are the resistance and inductance of grid filter, $\omega$ is the grid frequency 100π(), $C_{dc}$ is the dc link capacitance,$k_{p1}$&$k_{p2}$ are the values of proportional control,$k_{I1}$&$k_{I2}$ are the values of integration control and $V_{dc,ref}$&$I_{q,ref}$ are the reference input of grid side control that can calculated as:

$$V_{dc,ref} = \frac{P_m}{I_{dc}}$$

(19)

$$I_{q,ref} = \frac{2P_m}{3V_q}$$

(20)



The values of PI control can be calculated as

$$k_{p1} = 2 * I_{q,ref} k_{I1} = \frac{I_{q,ref}}{50}$$

(21)

$$k_{p2} = 2 * V_{dc,ref} k_{I2} = \frac{V_{dc,ref}}{50}$$

(22)

## IV. DYNAMIC STABILITY ANALYSIS USING LYAPUNOV FUNCTION

The simplified circuit shown in Fig. 6 is getting by concentrating on the dc side of the PV system shown in |Fig. (3) and neglecting all the internal resistive components and considering that the circuit is in off mode. Applying Kirchhoff's current law at nodes 1 &2 of Fig. 6

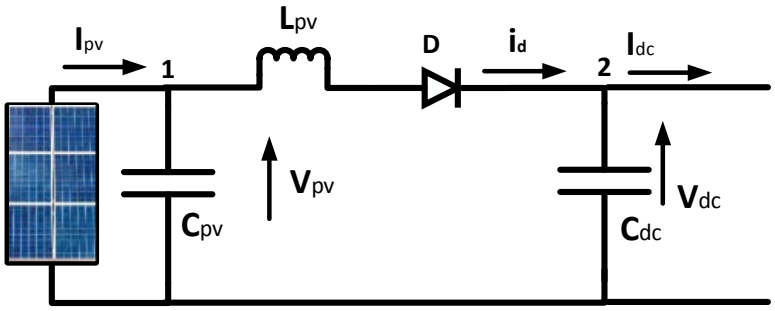


Fig. 6 PV system on off mode of dc side

$$I_{ph,pv} - I_{0,\mathrm{pv}}\left(\mathrm{e}^{\left(\mathrm{V_{dc}}+\mathrm{L_{pv}}\frac{\mathrm{di}}{\mathrm{dt}}\right)} - 1\right) - \mathrm{i} - \mathrm{I_{C_{pv}}} = 0 \quad (23)$$

$$\mathrm{i} - \mathrm{C_{dc}}\frac{\mathrm{dV_{dc}}}{\mathrm{dt}} - \frac{P_{dc}}{V_{dc}} = 0 \quad (24)$$



Where

$$I_{0,\mathrm{pv}} = N_p I_0$$

$$I_{ph,pv} = N_p I_{ph}$$

$$= \frac{1}{\mathrm{V_t}}$$

$\mathrm{I_{C_{pv}}}$ is the current passing through$\mathrm{C_{pv}}$and is calculated as

$$\mathrm{I_{C_{pv}}} = \mathrm{C_{pv}}\frac{\mathrm{dV_{pv}}}{\mathrm{dt}} \quad (25)$$

The duty cycle (D) of the boost converter is given in Eq. (26) where the DC link voltage must be maintained at constant reference value.

$$V_{pv} = (1 - D)V_{dc} \quad (26)$$

By substituting the value of $V_{pv}$ from Eq. (26) into Eq. (25)

$$I_{C_{pv}} = C_{pv}(1 - D)\frac{dV_{dc}}{dt} \quad (27)$$

Substitute the value of $V_{pv}$ in Eq. (25), then replacing the value of $\frac{dV_{dc}}{dt}$ from Eq. (24) into Eq. (27) and following some manipulation,

$$I_{C_{pv}} = \frac{C_{pv}(1-D)}{C_{dc}}(i - \frac{P_{dc}}{V_{dc}}) \quad (28)$$

$$\frac{di}{dt} = \frac{1}{L_{pv}}\left[\frac{1}{}\ln\left(\frac{I_{ph,pv}-i-I_{C_{pv}}}{I_{0,pv}} + 1\right) + V_{dc}\right] \quad (29)$$

$$\frac{dV_{dc}}{dt} = \frac{1}{C_{dc}}\left[i - \frac{P_{dc}}{V_{dc}}\right] \quad (30)$$



Let $f_1 \& f_2$ as [18]

$$f_1 = \frac{1}{L_{pv}}\left[\frac{1}{}\ln\left(\frac{I_{ph,pv}-i-I_{C_{pv}}}{I_{0,pv}} + 1\right) + V_{dc}\right] \quad (31)$$

$$f_2 = \frac{1}{C_{dc}}\left[i - \frac{P_{dc}}{V_{dc}}\right] \quad (32)$$

Lyapunov function ($V$) for PV system can be written [11] as

$$V = [f_1 \quad f_2]\begin{bmatrix} f_1 \\ f_2 \end{bmatrix} \quad (33)$$

$$V = {f_1}^2 + {f_2}^2 \quad (34)$$

The derivative of Eq. (34) can be written as

$$\dot{V} = 2(f_1 \dot{f_1} + f_2 \dot{f_2}) \quad (35)$$

The Jacobian matrix of the system ($A_{pv}$) can be obtained according to [11]

If the value of the determinant of The Jacobian matrix of the system $A_{pv}$ is negative, then derivative of the Lyapunov function ($\dot{V}$) has a negative value, then the system is stable, and vice versa.

$$A_{pv} = \begin{bmatrix} \left(\frac{1}{L_{pv}^2\alpha^2} * \frac{1}{I_{ph,pv}-i-I_{C_{pv}}} ln\left(\frac{I_{ph,pv}-i-I_{C_{pv}}}{I_{0,pv}}+1\right) + \frac{V_{dc}}{L_{pv}^2\alpha}\frac{1}{I_{ph,pv}-i-I_{C_{pv}}+I_{0,pv}}\right) & \left(\frac{V_{dc}}{L_{pv}^2} - \frac{1}{L_{pv}^2\alpha} * ln\left(\frac{I_{ph,pv}-i-I_{C_{pv}}}{I_{0,pv}}+1\right)\right) \\ \left(\frac{i}{C_{dc}^2 V_{dc}} - \frac{P_{dc}}{C_{dc}^2}\right) & \left(\frac{iP_{dc}}{C_{dc}^2 V_{dc}^2} - \frac{P_{dc}^2}{C_{dc}^2 V_{dc}^3}\right) \end{bmatrix} \quad (36)$$



## V. SIMULATION RESULTS

Fig. 7 depicts the Matlab/Simulink model of the complete system. The performance of the grid-connected PV system has been simulated with the zero dynamic controllers to enhance the dynamic stability. The most important parameters of the system are given in "Table 1". In order to investigate the effectiveness of the control algorithms, a dynamic simulation is done with different solar irradiance and temperatures. In all case, the gains of the PI controllers depend on the reference values of the dc link voltage and current grid.

These reference values are calculated from Eqs. (19) to (22). Thus, the gain of PI controllers is updated automatically with the change in temperature and radiation of the sun [18].

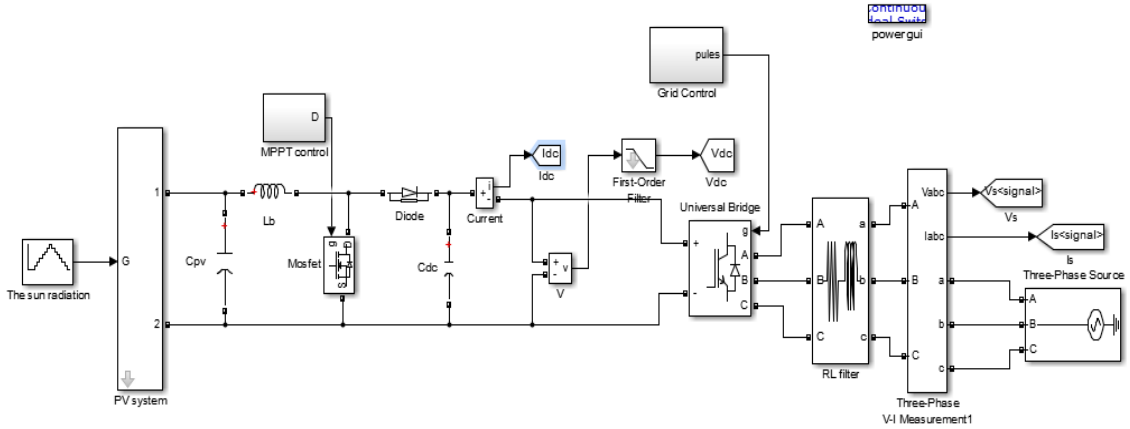


Fig. 7 Simulink block diagram of the PV system



"Table 1.Parameters for simulation"

| | | | |
|---|---|---|---|
| PV module type | SPR-305-WHT Solar Panel, Sun Pow | Number of series modules | $N_s$ =10 |
| Module output power at MPP | 305 W | Number of parallel modules | $N_p$ =164 |
| Module output voltage at MPP | 54.7 V | PV system output power at MPP | 500.2 KW |
| Module output current at MPP | 5.58 A | PV system output voltage at MPP | 547 V |
| Open circuit voltage | $V_{oc,n}$ = 64.2 V | PV system output current at MPP | 915.12 A |
| Short circuit current | $I_{sc,n}$ = 5.96 A | Boost converter | |

| | | | |
|---|---|---|---|
| The normal cell operating temperature | NCOT = 47 Celsius | The maximum of output dc link voltage | $V_{dc}$ = 1100 V |
| The nominal temperature | $T_n$ = 25 Celsius | Switching frequency | 5 KHz |
| The diode ideality constant | A = 1.3 | Capacitance of output PV system | $C_{PV}$ = 0.18 F |
| The open circuit voltage temperature coefficient | $K_v$ = -176.6 mV/C° | Capacitance of dc link | $C_{dc}$ = 0.008 F |
| The short circuit current temperature coefficient | $K_I$ = 3.5 mA/ C° | Inductance of boost converter | $L_b$ = 0.000018 H |
| | | Grid side | |
| | | Grid voltage | $V_s$ = 700 $v_{rms}$ |
| | | Switching frequency of grid control | 5 KHz |
| | | Grid filter | R = 2 Ω & L = 0.003 H |
| | | Grid frequency | $\omega$ = 100π rad/ sec |



In order to investigate the effectiveness of the control algorithms, a dynamic simulation is done with solar irradiance is changed from 700 $w/m^2$ to 1000 $w/m^2$ at 0.5 sec. and is dropped from 1000 $w/m^2$ to 700 $w/m^2$at 0.82 sec at different values of $C_{PV}$as shown in fig. 8. Fig.8(a), (b) and (c) show the simulation results of the first control stage (the boost converter) with the values of $C_{PV}$ are 0.08, 0.18 and 0.28 F; respectively. From the figures, it is concluded that the value of the $C_{PV}$ has a great effect on the speed and the performance of the proposed control. With the value of $C_{PV}$is 0.08, the PV voltage reaches its settle value faster but with a more ripples. While when the value of the $C_{PV}$ is 0.28, the PV voltage takes more time to reach its settle value with little ripples. It is shown that with the value of $C_{PV}$ is 0.18, the performance and control time are better, so it is used in this study. As shown from the fig. 8(b) the effect of solar irradiance on the array terminal voltage is small compared to its effect on output current. This is expected from the I-V characteristics of the PV array.

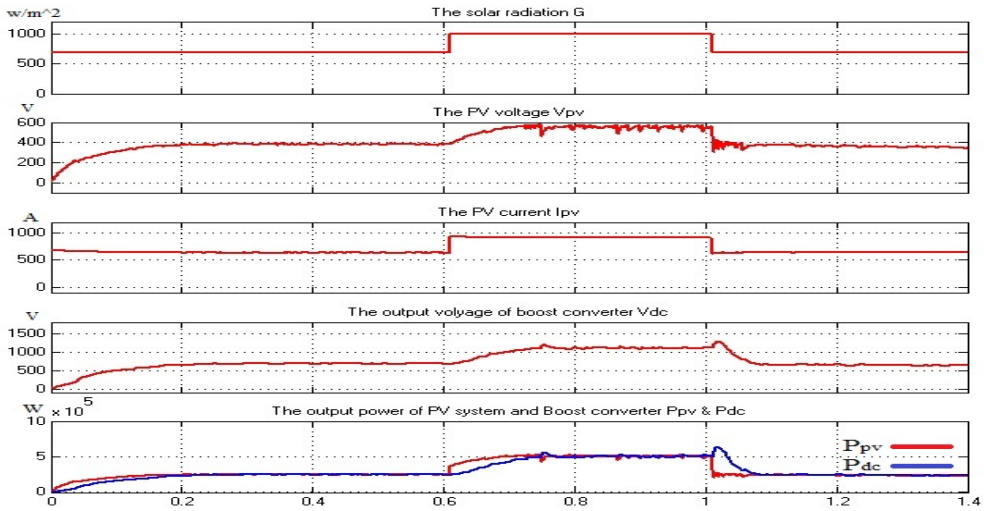


**A)** $C_{PV}$ =0.08 F

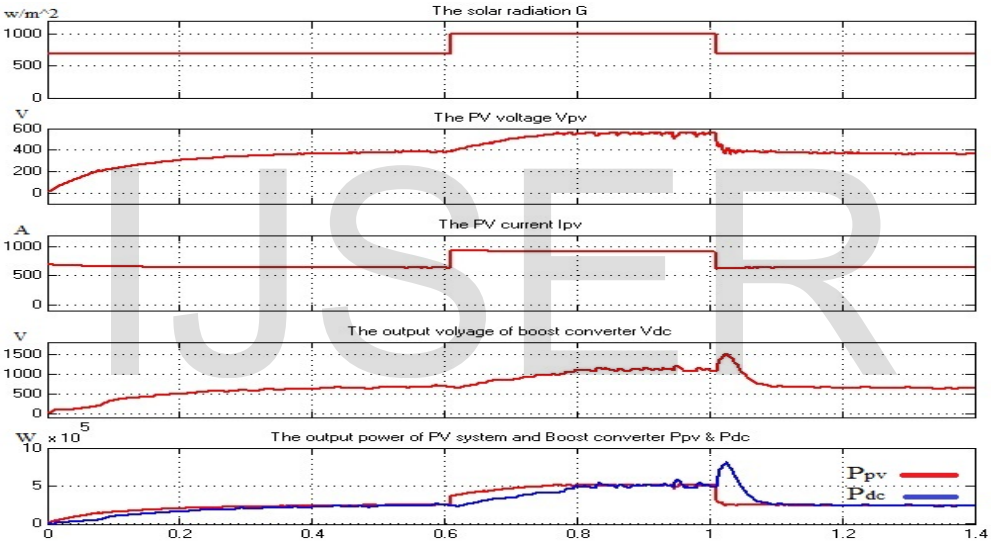


**B)** $C_{PV}$ =0.18 F

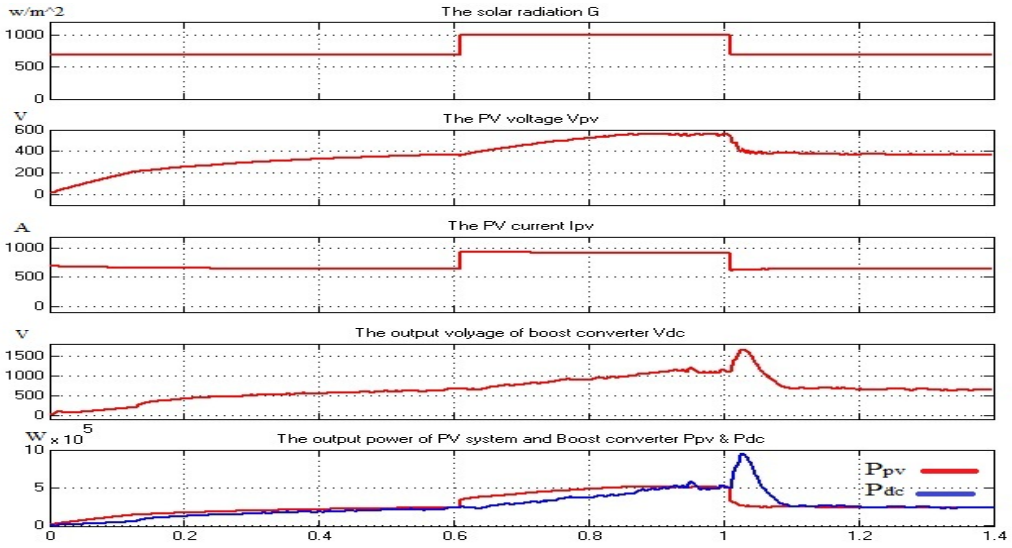


**C)** $C_{PV}$ =0.28 F

Fig. 8 The simulation results of the first control stage (the boost converter) at different values of $C_{PV}$

Fig. 9 shows the dynamic behaviors of the three phase grid voltage and grid current at the PCC. It is expected that the grid voltage waveform does not change during the transient since it is set by the AC network, whilst the grid current amplitude decreases in response due to the sudden change of the PV generated power.

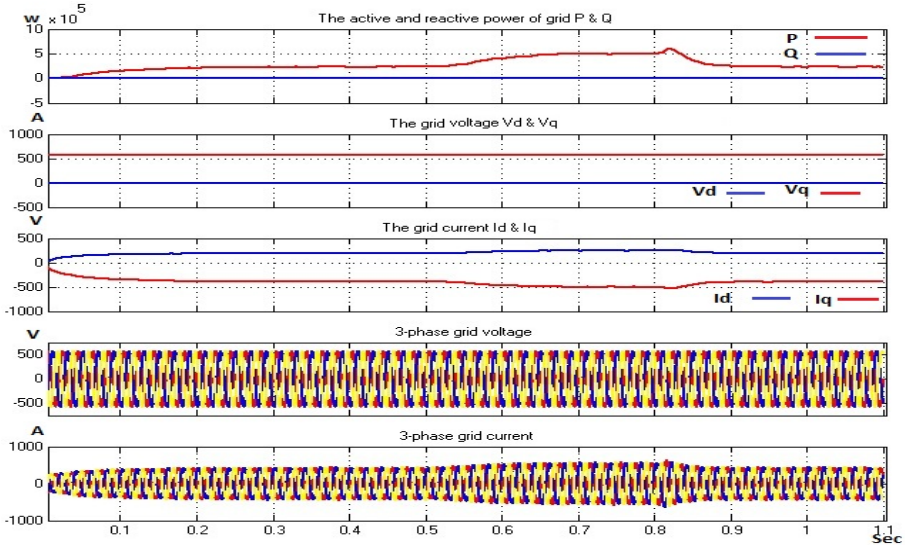


Fig. 9 The simulation results of the second control stage

In a practical PV system, the atmospheric condition changes continuously for which there exist variations in cell working temperature as well as in solar irradiance. The performances of the proposed controller with

the change in atmospheric conditions are shown in Fig. 10. The irradiance changes gradually from 300w/$m^2$ until reaching to the standard atmospheric condition where the value of solar irradiation is considered as 1000w/$m^2$ then decreases gradually to 300w/$m^2$. The ambient temperature is considered as 298 K. Fig. 10(a) shows the simulation results of the first control stage (the boost converter) while Fig.10 (b) illustrates the second control stage simulation results. It can conclude from fig. 10(a) that there is a very small loss between the PV and boost converter powers. Fig. 10(b) shows the amount of power delivered to the grid which is changed with the variation of radiation while the grid voltage waveform does not change and the reactive power is zero.

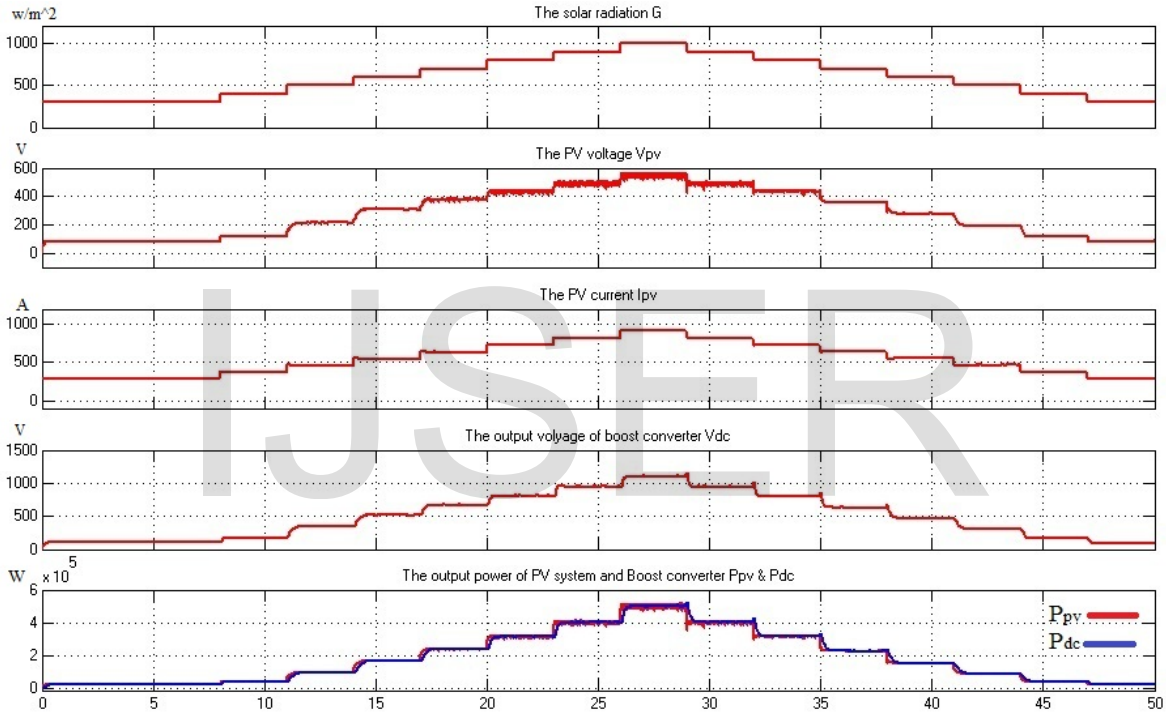


**a)** The simulation results of the first control stage (the boost converter)

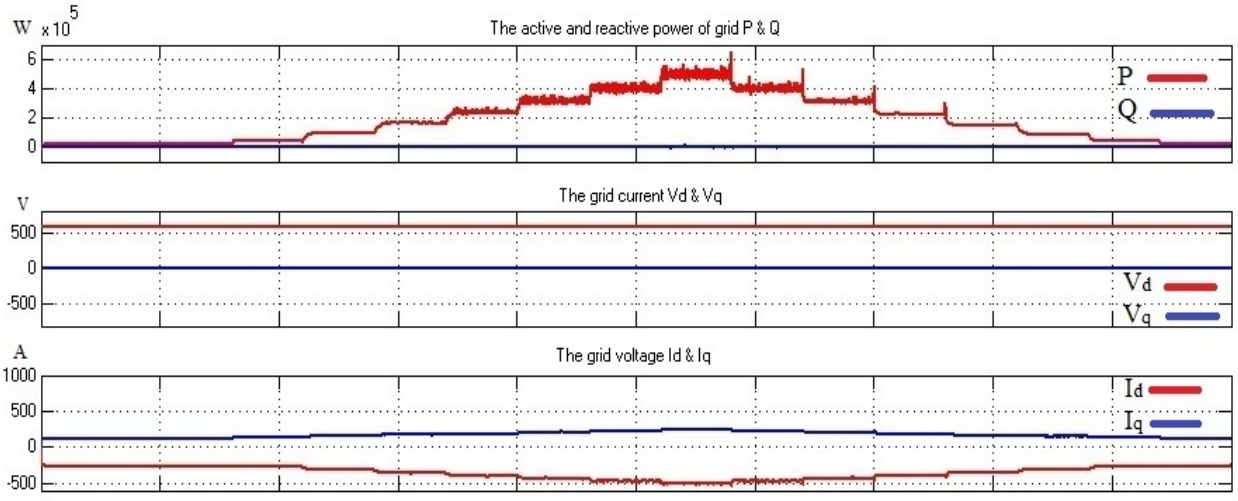


**b)** The simulation results of the second control stage

Fig. 10 Simulation results of the proposed controller at ambient temperature 298 K.

Fig. 11 demonstrates the same simulation results at temperature 313 K. From the figure, it is seen that with the increase of the temperature, the output current , voltage and power of the PV system are increased.



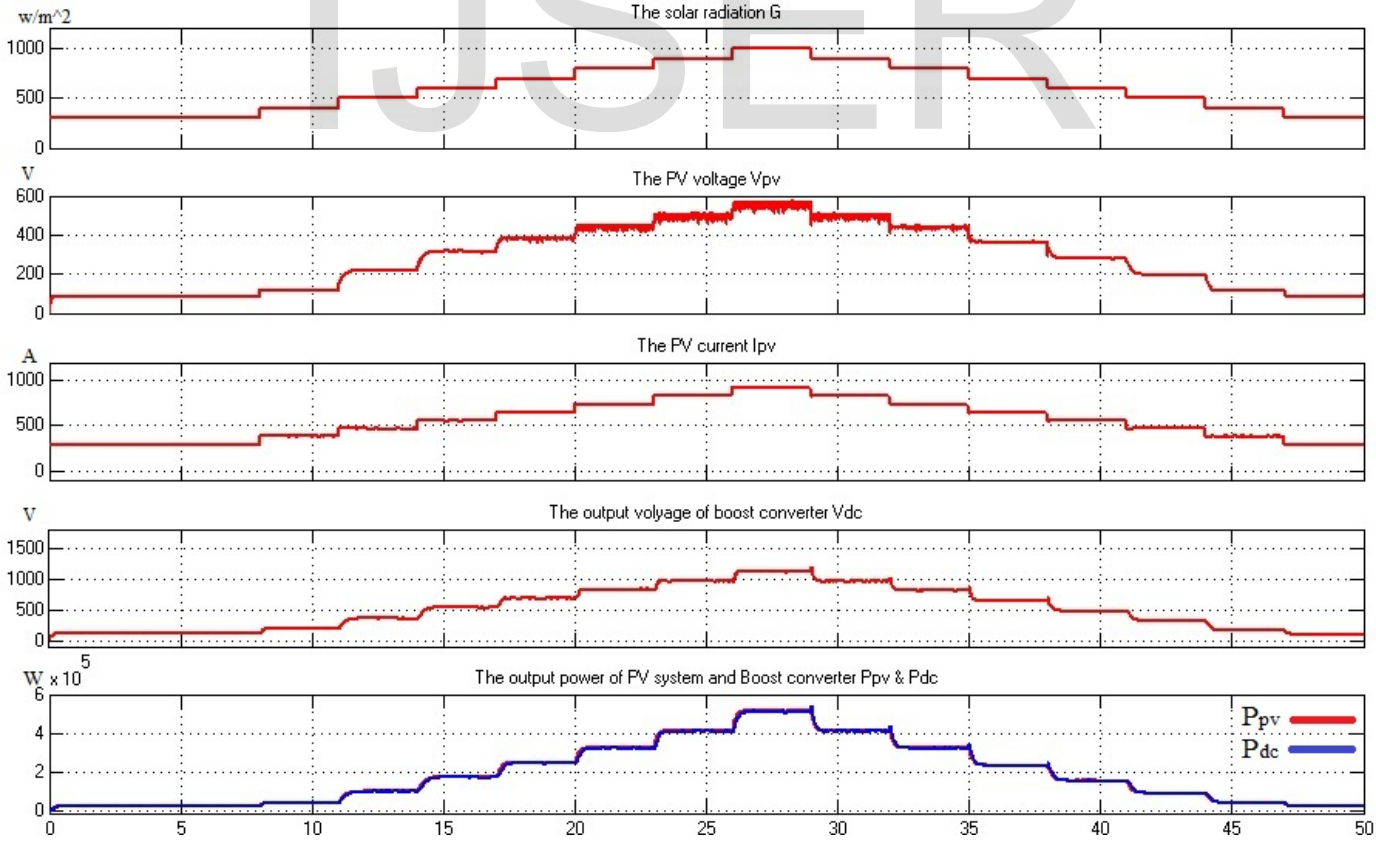


**a)** The simulation results of the first control stage (the boost converter)

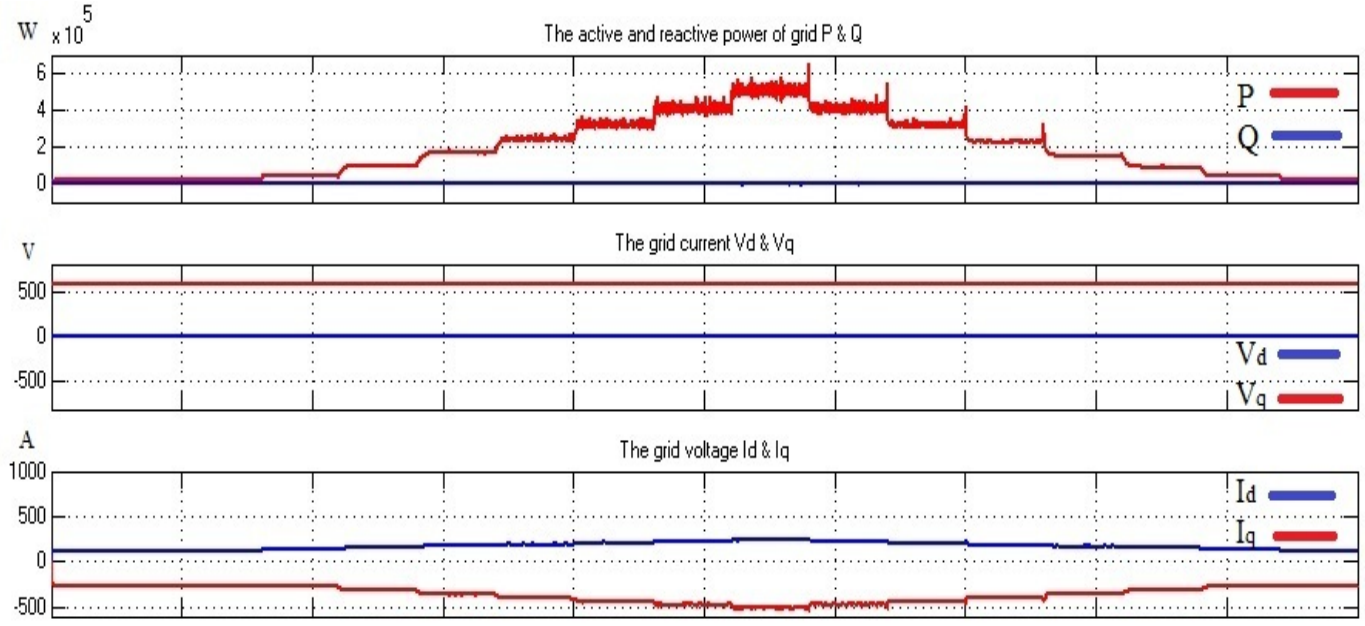


**b)** The simulation results of the second control stage

Fig. 11 Simulation results of the proposed controller at ambient temperature 313 K.

The value of $\dot{V}$ and the statues of the PV system at different irradiance are shown in "Table 2". From the table it is concluded that the system is stable as the values of $\dot{V}$ at different irradiance are negative.

"Table 2. Stability Assessment using Lyapunov function"

| G | $I_{ph,pv}$ | $I_{0,\mathrm{pv}} * 10^{-82}$ | $\mathrm{V_{dc}}$ | $I_{dc}$ | i | $\mathrm{V_{pv}}$ | D | $\dot{V} * 10^{15}$ |
|---|---|---|---|---|---|---|---|---|
| 300 | 282.55 | 1.16 | 103.5 | 231.5 | 232 | 86.3 | 0.1662 | -2.3188 |
| 400 | 377.4 | 1.59 | 177 | 248 | 248.5 | 117.7 | 0.335 | -5.4804 |
| 500 | 462.57 | 2.17 | 352 | 286.5 | 287 | 219.5 | 0.3764 | -5.193 |
| 600 | 550 | 2.94 | 524.5 | 326.5 | 327 | 313 | 0.4032 | -20.378 |
| 700 | 640.23 | 3.96 | 677 | 361.5 | 362 | 383.1 | 0.4341 | -26.918 |

| | | | | | | | | |
|---|---|---|---|---|---|---|---|---|
| 800 | 732.56 | 5.29 | 817 | 392.5 | 393 | 441.2 | 0.46 | -32.922 |
| 900 | 826 | 7.03 | 964 | 424.5 | 425 | 498.5 | 0.4829 | -39.225 |
| 1000 | 918 | 9.27 | 1100 | 461.5 | 462 | 547 | 0.5027 | -45.057 |

## VI. CONCLUSION

In this paper the Lyapunov function and a modified zero dynamic control scheme are presented to analyze the performance of a three-phase grid-connected PV system and to enhance the dynamic stability limit with the change in temperature and radiation of the sun. The boost converter is controlled using the modified INC algorithm to achieve the MPP to give the maximum efficiency of the PV system. The value of the dc link voltage between the two converters and the current values of the grid are used to set the values of the PI controller of the grid. The simulation results demonstrate that the controller performs better under varying atmospheric conditions.



## VII. REFERENCES

[1] Azza ElDesouy "Security constrained generation scheduling for grids incorporating wind, photovoltaic and thermal power" *Electric Power Systems Research*, 116 (1) ,pp. 284-292, 2014.

[2] AissaChouder, Santiago Silvestre, Nawel Sadaoui and Lazhar Rahmani " Modeling and simulation of a grid connected PV system based on the evaluation of main PV module parameters" Elsevier / Simulation Modeling Practice and Theory, 20(1), pp. 46–58, January 2012.

[3]Darren M.Bagnall and Matt Borel " Photovoltaic technologies" Elsevier Energy Policy 36 , pp. 4390–4396, 2008.

[4] T.M. Razykov , C.S. Ferekides, D. Morel, E. Stefanakos, H.S. Ullal, H.M. Upadhyaya " Solar photovoltaic electricity: Current status and future prospects " Elsevier/ Solar photovoltaic electricity: Current status and future prospects, 85(8), pp. 1580–1608, August 2011.

[5] RobertoFaranda andSoniaLeva " Energy comparison of MPPT techniques for PV Systems "WSEAS Trans. on Power Syst. 3,June 2008.

[6] Carlos Francisco González Toraya" Rafael Jiménez Castañeda, Juan Andrés Martín GarcíaandJuan Antonio LópezRamírez, Approach for locating and tracking the maximum power point of a photovoltaic generator using a centered differentiation method " Elsevier/ Sustainable Energy and Grids and Networks, 8, pp. 62–73, December 2016.

[7] IoanViorelBanu, RăzvanBeniugă and Marcel Istrate " Comparative analysis of the Perturb-and-Observe and incremental conductance MPPT methods " The 8th International Symposiumon Advanced Topics in Electrical Engineering, Bucharest, Romania,pp 23-25, May 2013.

[8] David Taggart, Kei Hao, Robin Jenkins, and Rick VanHatten " Power factor control for grid-tied photovoltaic solar farms proceedings of the 3rd Annual Protection " Automation and Control World Conference Budapest, Hungary,pp 25–28, June 2012.

[9] VahanGevorgian and Barbara O'Neill " Advanced grid-friendly controls demonstration project forutility-scale PV power plants"NREL/TP-5D00-65368,January 2016.

[10] R. Yousefian and S. Kamalasadan " A Lyapunov function based optimal hybrid power system controller for improved transient stability "*Electric Power Systems Research*, 137, pp. 6-15, 2016.

[11] M. A. Mahmud, H. R. Pota and M. J. Hossain " Dynamic stability of three-phase grid-connected photovoltaic system using zero dynamic design approach "2(4), pp. 564 571, 2012.

[12] Marcelo Gradella Villalva, Jonas Rafael Gazoli, and Ernesto Ruppert Filho "Comprehensive approach to modeling and simulation of photovoltaic arrays " IEEE Trans. on Power Electronics,24(5) MAY2009.

[13] Aissa Chouder , Santiago Silvestre , Nawel Sadaoui and Lazhar Rahmani " Modeling and simulation of a grid connected PV system based on the evaluation of main PV module parameters" Elsevier, Simulation Modeling Practice and Theory 20, pp. 46–58, 2012.

[14] Soumy adeep Nag and Namitha Philip '' Off – line optimization of strategic and design parameters of a hybrid stand-alone wind/solar/fuel cell/battery system, IOSR Journal of Computer Engineering (IOSR-JCE), 16 (5), pp. 13-26, Sep – Oct.2014.

[15] Tarak Salmi, Mounir Bouzguenda, Adel Gastli and Ahmed Masmoudi '' MATLAB/Simulink based modeling of solar photovoltaic cell, International Journal of Renewable Energy Research, 2 (2), 2012.

[16] N. Hamrouni and A. Chérif '' Modeling and control of a grid connected photovoltaic system'' Revue des Energies Renouvelables,10(3),pp.335 – 344 , 2007.

[17] M.Abdulkadir, A. S. Samosir, A. H. M. Yatim and S. T. Yusuf '' A new approach of modeling, simulation of mppt for photovoltaic system in simulink model'' ARPN Journal of Engineering and Applied Sciences, 8(7), JULY2013.

[18] WWW.sunpowercorp.com/panels for details/ 305 solar panel.